Asian Journal of Chemistry Vol. 19, No. 1 (2007), 10–26

Influence of Trace Elements in Cemented Carbide Production

E. ALIZADEH
Department of Chemistry, Faculty of Sciences, Guilan University, P.O. Box 1914, Rasht, Iran
E-mail: homayoon152000@yahoo.com

Trace elements ranging between 10 and 200 ppm, added to tungsten blue oxide prior to reduction, appear to have a considerable influence on the reduction kinetics and properties of tungsten powders. Marked effects on the grain growth, shape and size of the tungsten crystallites, the Scott density, the grain size distribution and the degree and solidity of agglomerations can be observed even though the impurity elements are partially volatilized during reduction. In order to determine the effects of interactions between impurities, powders containing more than one trace element at a time were tested. The amount of impurity elements present in tungsten powders after reduction can be further reduced by a carburization reaction. The final concentration of impurities remaining in the tungsten carbide after carburization of the tungsten powder depends on the nature of the element and of the chemical compound added as well as on the time and temperature of the heating cycle. Distinct influences of the trace impurities on the grain growth and on the properties of tungsten carbide powder were observed. In tungsten carbide powders, grain size and grain size distribution, as well as the size of the single crystalline domains within the polycrystalline tungsten carbide grains, are influenced by impurities. The oxygen content and milling behaviour of the powder also depend on foreign elements, even though their concentration is very low in most cases after carburization. Impurities also appear to have a remarkable influence on the grain growth of tungsten carbide crystals during liquid phase sintering in molten cobalt and consequently on the final structure of cemented carbides.

Key Words: Trace elements, Cemented carbide.

INTRODUCTION

The properties of cemented carbides greatly depend on their chemical composition and their microstructure formed during liquid phase sintering. For all applications of tungsten carbide-cobalt hard metals, utmost homogeneity in tungsten carbide grain size and distribution in the binder phase is desirable. During sintering, the size and shape of the particles are altered. The coarsening of the tungsten carbide grains can be influenced by the sintering parameters, such as temperature, time, atmosphere, heating and/or cooling rate and milling conditions. Another important set of parameters is linked with the raw materials (particle size, grain size distribution, etc.). A decrease in interface energy between tungsten carbide and binder phase is assumed to be the driving force for this grain growth[1–3].

Grain growth during sintering of tungsten carbide-cobalt hard metals can occur in two ways: (1) a uniform increase of the average tungsten carbide crystal size (continuous grain growth); (2) a preferential growth of certain tungsten carbide grains (discontinuous or local grain growth).

These growth modes do not compete with each other and may occur simultaneously. Generally, continuous grain growth should be kept at a minimum, whereas discontinuous grain growth should be avoided completely.

Previous investigations indicated that the nature of the raw materials for tungsten carbide production, such asd tungstic acid (H_2WO_4), tungsten oxide (WO_3) or ammonium paratungstate ($(NH_4)_2O{\cdot}2WO_3{\cdot}5H_2O$), can influence the sintering behaviour of the carbide powders[4]. More recent publications refer to the influence of traces of foreign elements present in the oxide stage on the sintering behaviour[5–10]. Controlling grain size and grain size distribution of tungsten carbide powders used is of utmost importance[11, 12]. Discrepancies in literature may be related to the difficulty of an exact quantitative determination of all relevant powder parameters.

The present paper deals with the origins of discontinuous grain growth occuring with fine grained tungsten carbide powders (0.6–1.5 μm average grain size).

EXPERIMENTAL

Table-1 shows the elements, their concentrations and the nature of chemical compounds that were added. These compounds were added to the blue oxide either as an aqueous solution or in the case of low solubility, as an aqueous suspension. The resulting slurry was dried and homogenized.

After the addition of the impurities the blue oxide samples were reduced by hydrogen under technical conditions in a multi-tube pusher-type furnace as described in literature[5]. Two sets of conditions, differing in time, temperature and boat load, were used which would result in tungsten powders of 0.7 or 5.5 μm under normal industrial production conditions (no dopant added).

Only 1 tube out of 14 of a reduction furnace[5] was used for the doped material. The powder was pushed through the furnace in 3 or 4 boats together with boats of the normal production. In order to avoid mutual contamination by evaporation of impurities, boats loaded with tungsten powders containing different impurities were never reduced during the same experiment.

Carburization: Tungsten powders which had been mixed with lampblack by ball milling for 12 h were carburized in covered graphite boats at 1600°C in dry hydrogen. The resulting tungsten carbide was deagglomerated for 10 min in a ball mill and screened (100 μm).

Preparation of cemented carbide samples: Tungsten carbide and 10g cobalt (wt %) were mixed under cyclohexane in a planetary ball mill for 1 h. After evaporation of cyclohexane, test specimens (50 × 50 × 5 mm) were pressed

(20 kN/cm^2), pre-sintered in a hydrogen atmosphere for 1 h at 900°C and sintered under vacuum (5×10^{-4} mbar) at 1430°C for 1 h.

TABLE-1
ELEMENTS ADDED TO BLUE OXIDE

Doping element	Concentration (ppm)	Compound added	Doping element	Concentration (ppm)	Compound added
Li	200	LiOH	Mg	150	$Mg(NO_3)_2$
Li	100	LiOH	Ca	150	$Ca(NO_3)_2$
Li	50	LiOH	Ba	200	$Ba(NO_3)_2$
Li, B	300, 150	Li_3BO_3	B	200, 150	H_3BO_3, Li_3BO_3
Na	200	NaOH	Al	200	$Al(NO_3)_3$
Na	100	NaOH	Si	100, 120	SiO_2, $12WO_3$, Na_2SiO_3
Na	50	NaOH	Sn	100	$SnSO_4$
Na, F	100, 80	NaF	P	100, 200	PO_3, $12WO_3$, Na_3PO_4
Na, Si	200, 120	Na_2SiO_3	As/Sb/Bi	Je 100	H_3AsO_4, $SbCl_3$, $Bi(NO_3)_3$
Na, P	140, 200	Na_3PO_4	Ni	100	$Ni(NO_3)_2$
Na, Al, U, F	150, 85, 90, 400	Na_3AiF_6	Cu	100	$Cu(NO_3)_2$
K	200	KOH	Zn	100	$Zn(NO_3)_2$
K	100	KOH	U	100	$UO_2(NO_3)_2$
K	50	KOH			

RESULTS AND DISCUSSION

Change in concentration of trace elements during reduction and carburization: The respective concentrations of doping elements in the three stages (blue oxide, tungsten powder and tungsten carbide powder) are shown in columns 2, 3 and 4 of Tables 2 and 3.

Behaviour of various impurities during reduction of tungsten-blue oxide: Tungsten blue oxide shows ion exchanger properties when in contact with chemical compounds dissolved in aqueous solutions. This means that chemical bondings can exist between polymeric tungstate species and the ions of the dopant at the surface of blue oxide particles. Not only cations can be bound due to the heteropolar character of the polymeric tungstate, but also anions, especially those which form heteropolytungstate compounds, such as silicates, phosphates or arsenates. During heating in the reduction furnace to temperatures of between 700° and 1000°C in a hydrogen atmosphere, different reactions were observed.

Elements, totally removed, independently of reduction conditions: Zinc compounds were reduced to metallic zinc (m.p./b.p. 419/907°C). Sulphur and halogens were transformed into their respective hydrogen compounds which are all highly volatile. For these elements the reduction step is also very important for purification reasons.

Elements, partly evaporated, dependent on the reduction conditions: The evaporation rate depended on the chemical nature of the element and on the reduction conditions. Metallic potassium and sodium, having boiling points of 760 and 883°C respectively, were more rapidly removed than lithium (1330°C). The higher the reduction temperature, the higher the degree of evaporation.

Alkali metal tungstates, formed during doping were firstly reduced to low melting point tungsten bronzes $M_2O{\cdot}xWO_3$ [2, 3, 5] which formed molten neck-like connection between the tungsten grains. Later, during reduction these bronzes were decomposed to tungsten and alkali oxide according to eqn. (1).

$$M_2O{\cdot}xWO_3 \xrightarrow{H_2} M_2O + xW + 3xH_2O \qquad (M = \text{alkali metals}) \qquad (1)$$

The latter reacted as shown in eqn. (2).

$$xM_2O + W \longrightarrow WO_x + 2xM^{\bullet} \qquad (2)$$

While Me was partially removed by the H_2-stream, it partially reacted again with H_2O to reform its oxide according to (3).

$$2M + H_2O \longrightarrow M_2O + H_2 \qquad (3)$$

Finally, the tungsten suboxide, formed from the bronzes[1], was also reduced to tungsten according to (4).

$$WO_x + xH_2 \longrightarrow W + xH_2O \qquad (4)$$

and thus formed solid tungsten necks between the tungsten grains[4]. For this reason alkali-doped blue oxides resulted in highly agglomerated tungsten powders having comparatively low Scott densities.

The mechanism of volatilization for B, Si, P is not yet completely understood. It can be assumed, however, that the partial pressure of water vapour is more important for the evaporation of these elements than is temperature. The higher the water vapour concentration, the more the equilibrium shifted towards the oxide side. Contrary to alkali metals, the oxides of these elements are more volatile than the pure elements.

All three elements remained in the tungsten powder under reduction conditions which gave 0.7 μm powders, whereas they partially evaporate under 5.5 μm conditions. Boron and phosphorus were less stable than silicon. As already mentioned by Lassner[7], heteropolytungstate bondings, as formed with phosphates and silicates, are extremely stable during the reduction process.

Elements showing no change in their concentration during blue oxide reduction: The alkali-earth metals, tin and aluminium, form stable oxides, which cannot be reduced at temperatures between 700 and 1000°C in the presence of hydrogen and tungsten. For this reason, magnesium, even though it is a highly volatile element, did not show any decrease in concentration during the reduction operation. Metals such as copper and nickel were reduced to the metallic form and diffused into the tungsten grains to form solid solutions.

Change in evaporation rates of impurities due to the mutual interactions: Distinct interaction influences could be observed with some elements as shown in Figs. 1 and 2. Fig. 1 shows the rate of evaporation of lithium during reduction for

TABLE

PROPERTIES OF PURE AND DOPED W-, WC-POWDERS AND WC/10 wt% FOR WC OF 0.7

Doping elements				Grain size (Fisher sub sieve size)						Sintered structure		Coarse particles Cu-embedded	Agglomeration (%)	
Elements	Concentration			as supplied (μm)			lab-milled (μm)			Grain growth	Structure		W	WC
	WO_{3-x}	W	WC	W	WC	Δ6–5	W	WC	Δ9–8					
1	2	3	4	5	6	7	8	9	10	11	12	13	14	15
None	—	—	—	1.04	1.92	+0.88	0.49	0.92	0.43	D	–	–	51	52
Na	200	96	40	1.60	1.20	–0.40	0.88	1.02	0.14		+	–	37	15
Na	140	120	<10	1.70	1.38	–0.32	0.76	1.26	0.50	C+	–	–	55	7
P	200	150	129											
Na	200	190	14	1.08	1.60	+0.52	0.89	1.21	0.32	C+	–	–	18	24
Si	120	140	115											
Na	100	126	10	1.75	1.61	+0.46	0.79	1.20	0.41	C	–	–	31	26
F	80	<10	<10											
Na	150	152	18	1.02	1.21	+0.19	0.70	0.97	0.27	D	–	–	31	20
Al	85	88	116											
U	90	95	97											
F	400	<10	<10											
Li	200	220	78	1.75	1.33	–0.42	1.14	1.31	0.17	D	–	–	35	2
Li	100	146	13	1.31	1.66	+0.35	0.78	1.12	0.34	D	–	–	41	33
B	150	50	50											
K	200	178	16	1.15	1.80	+0.65	0.81	1.13	0.32	C+	–	–	30	37
Mg	150	190	30	0.85	1.54	+0.69	0.55	1.09	0.54	C	–	–	35	29
Ca	150	190	132	1.06	1.06	—	0.54	0.94	0.41	C	–	–	49	10
Ba	200	240	190	0.84	1.64	+0.08	0.55	1.02	0.47	D+	–	–	35	38
B	200	250	50	1.30	1.11	–0.19	0.39	0.70	0.31	D	–	–	70	37
Al	200	340	168	0.88	1.27	+0.59	0.50	0.70	0.20	D+	–	–	27	45
Si	100	100	110	1.19	0.99	–0.02	0.54	0.65	0.11	D	–	–	55	34
P	100	146	121	1.08	1.44	–0.36	0.60	0.48	0.38	D+	–	–	44	32
Zn	100	<10	<10	0.81	2.10	+1.29	0.58	0.85	0.27	D	–	–	28	60
Cu	100	100	108	0.89	1.58	+0.89	0.62	1.00	0.38	D	–	–	30	37
Ni	100	188	118	0.99	2.10	–1.11	0.65	1.00	0.35		+	–	34	52
C	100	118	110	1.29	0.89	–0.40	0.59	0.62	0.03	D	+	–	54	30
R.E.	93	82	90	0.83	2.10	+1.27	0.65	1.15	0.50		+	–	22	45
Sn	100	150	<10	1.00	1.44	+0.44	0.64	1.12	0.48		–		36	22
As	100	50	36	2.10	1.13	–0.97	0.41	0.70	0.29	D	–	+	80	38
Sb	100	200	150											
Bi	100	250	250											

Abbreviations: R.E. —Rare earth metals
D —Discontinuous grain growth
C —high discontinuous grain growth
D^{+} —high continuous grain growth

-2
Co CEMENTED CARBIDES (POWDERS REDUCED UNDER CONDITIONS
µm GRAIN SIZE)

Scott density (g/inch^3)		Grain size distribution						Carbon content (%)				Oxygen content (ppm)	
W	WC	W (µm)			WC (µm)			Diff. to add'n	Total	Free	Bound	W	WC
		<0.5	<1.0	>2.0	<0.5	<1.0	>0.2						
16	17	18			19			20				21	
38	41	72	95	4	57	87	7	–0.09	6.11	0.03	6.08	2420	550
37	38	18	72	2	20	72	5	–0.03	6.17	0.30	5.87	710	790
37	36	23	80	3	21	70	4	–0.06	6.14	0.08	6.06	1460	480
36	42	17	81	4	27	80	4	+0.01	6.22	0.13	6.09	1070	420
37	39	25	82	4	20	75	5	+0.03	6.23	0.13	6.10	1020	400
34	39	37	84	3	50	85	6	–0.08	6.12	0.05	6.07	1210	770
56	33	23	72	4	19	66	7	–o.05	6.14	0.16	5.99	1030	850
38	45	60	90	4	29	80	4	–0.06	6.13	0.05	6.08	1480	450
36	43	28	80	5	27	80	8	–0.02	6.18	0.11	6.07	950	490
38	39	66	92	5	34	85	7	–0.01	6.19	0.12	6.07	2490	470
37	41	43	87	4	27	81	6	–0.09	6.11	0.09	6.02	1660	610
37	42	65	92	5	45	88	5	–0.06	6.15	0.05	6.10	2140	600
55	37	77	92	4	57	86	9	–0.18	6.01	0.03	5.98	2950	930
46	42	71	92	3	51	86	8	–0.22	6.01	0.05	5.95	2720	1440
41	37	60	92	4	36	83	8	–0.13	6.07	0.39	5.78	2540	1390
41	42	65	92	5	46	85	9	–0.06	6.14	0.06	6.06	1710	570
38	46	70	54	4	63	89	9	–0.08	6.13	0.05	6.08	2290	620
38	44	59	90	5	43	87	5	–0.10	6.11	0.04	6.07	1910	600
38	44	61	36	2	48	88	7	–0.06	6.15	0.07	6.08	1470	520
39	36	49	90	5	57	88	7	–0.01	6.18	1.05	5.13	2119	1880
36	45	46	92	5	24	76	11	–0.05	6.16	0.05	6.11	1500	40
38	42	55	92	4	27	81	9	–0.04	6.17	0.08	6.09	1720	460
41	38	74	84	11	54	80	15	–0.18	6.01	0.01	6.00	3250	890

C$^+$ —high continuous grain growth
Structure$^+$ —homogeneous grain size of WC-particles in ceamented carbide
Structure$^-$ —inhomogeneous grain size of WC-particles in cemented carbide

TABLE
PROPERTIES OF PURE AND DOPED W-, WC-POWDERS AND WC/10 wt% FOR WC OF 5.5

Doping elements				Grain size (Fisher sub sieve size)						Size of single crystalline domains	Size distribution of s.c. domains	Micrograph of WC/Co	Crystal size of sintered WC	Agglomeration of W (%)
Elements	centration (ppm)			as supplied (μm)			lab-milled (μm)							
	WO_{3-x}	W	WC	W	WC	Δ6–5	W	WC	Δ9–8					
1	2	3	4	5	6	7	8	9	10	11	12	13	14	15
None	—	—	—	5.05	5.50	+0.15	4.94	0.93	+0.56	–	+	–	±	2.18
Na	200	10	40	1.60	1.20	+0.80	0.50	1.68	+1.50	+	–	–	–	6.25
Na	140	16	10	0.00	0.05	+1.05	8.50	0.58	+1.55	–	+	+	–	5.56
P	200	58	41											
Na	200	64	10	11.00	10.20	–1.30	10.65	2.80	–0.46	+	–	±	–	7.39
Si	130	100	20											
Na	100	10	10	11.00	10.20	–0.80	10.00	2.92	–0.20	±	–	+	–	9.09
F	80	<10	<10											
Na	150	152	18	10.00	10.25	+0.25	9.15	2.40	+1.15	–	+	–	–	8.50
Al	85	90	164											
U	90	75	80											
F	400	<10	<10											
Li	200	154	<10	16.50	13.45	–3.05	15.30	2.55	–1.85	+	±	–	–	7.27
Li	100	146	<10	20.00	10.70	–9.30	16.65	2.31	–5.95	±	–	–	–	16.75
B	150	5	5											
K	200	<10	<10	10.90	9.70	–1.20	10.25	2.90	–0.55	±	–	–	–	5.96
Mg	150	180	<10	4.73	5.50	+0.77	4.50	3.30	+1.00	±	–	–	±	15.40
Ca	150	220	45	4.40	5.30	+0.90	4.30	3.05	+1.00	–	+	–	–	2.27
Ba	200	240	30	5.30	5.80	+0.50	5.25	3.40	+0.65	±	–	+	+	0.90
B	200	20	25	4.70	5.00	+0.30	4.30	2.64	+0.70	–	+	±	–	8.51
Al	200	224	204	4.45	4.89	+0.54	4.20	3.18	+0.79	–	+	±	–	5.62
Si	100	72	98	4.45	4.85	+0.02	4.20	2.59	+0.65	–	±	–	–	5.62
P	100	33	31	5.20	5.40	+0.02	5.10	4.01	+0.30	±	–	–	+	1.92
Zn	100	<10	<10	5.10	5.83	+0.83	4.90	3.75	+0.93	+	±	±	+	5.77
Cu	100	140	44	5.50	4.81	–0.67	5.43	3.48	–0.60	±	–	–	+	1.27
Ni	100	128	110	5.60	5.30	–0.30	4.40	3.30	+0.90	–	–	–	±	21.4
C	100	80	45	5.00	5.60	+0.60	4.80	2.82	+0.70	–	+	–	–	2.00
R.E.	100	73	90	1.10	4.88	+0.28	4.55	3.08	+0.33	±	–	–	+	1.09
Sn	100	100	10	6.20	6.38	+0.28	5.90	3.05	+0.48	+	±	–	+	4.84
As	100	50	36	1.35	4.20	+0.25	3.50	2.69	+0.70	+	+	–	±	11.39
Sb	100	150	150											
Bi	100	250	25											

Abbreviations: R.E. —Rare earth metals
Column-1: + = large ± = medium; – = small
Column-2: + = homogeneous; – = heterogeneous

-3
Co CEMENTED CARBIDES (POWDERS REDUCED UNDER CONDITIONS
µm GRAIN SIZE)

Scott density (g/inch^3)		Grain size distribution					Carbon content (%)				Oxygen content (ppm)		Carburization
W	WC	W (µm)		WC (µm)			Diff. to add'n	Total	Free	Bound	W	WC	
		< 0.5	0.5–1.0	2/.0	10–20	> 15							
16	17	18		19			20				21		
47	63	18	3	33	2	0	–0.01	6.14	0.02	6.12	140	120	1x
58	94	1	50	21	18	4	–0.03	6.12	0.05	6.07	90	50	2x
58	88	0	35	20	28	0	–0.01	6.14	0.03	6.11	120	80	1x
53	96	00	43	23	10	1	–0.06	6.12	0.02	6.10	250	85	1x
54	93	3	29	18	13	2	–0.06	6.12	0.02	6.10	70	75	1x
52	91	2	36	22	17	4	0	6.15	0.05	6.10	270	70	2x
66	115	0	51	28	12	4	–o.09	6.18	0.11	5.05	480	100	3x
67	118	0	43	24	25	12	–0.12	6.07	0.39	5.68	250	80	1x
52	91	4	41	25	8	1	–0.10	6.11	0.02	5.09	70	90	1x
40	60	15	2	28	0	0	–0.05	5.13	0.01	6.12	230	130	1x
43	57	18	0	28	1	0	–0.05	6.11	0.02	6.09	180	180	1x
44	60	11	5	24	3	1	–0.06	6.12	0.04	6.10	160	120	1x
44	65	22	5	40	3	0	0	6.16	0.04	6.12	130	160	1x
58	59	20	3	29	3	1	–0.04	6.12	0.04	6.08	330	190	1x
54	67	19	4	32	2	1	–0.01	6.15	0.03	6.12	400	150	1x
40	58	8	8	18	2	0	–0.05	6.13	0.01	6.12	130	130	1x
41	62	10	4	24	0	0	–0.04	6.14	0.01	6.13	120	120	1x
41	63	8	8	22	3	1	–0.06	6.12	0.01	6.11	160	130	1x
40	57	15	9	31	1	0	–0.04	6.11	0.03	6.08	280	170	1x
50	60	11	16	25	2	0	–0.05	6.12	0.01	6.11	140	130	1x
43	66	14	0	29	1	0	–0.05	6.13	0.01	6.12	180	160	1x
47	69	11	12	24	5	0	–0.05	6.11	0.01	6.10	100	130	1x
51	53	30	3	44	1		–0.03	6.13	0.02	6.11	330	190	1x

Column-3: + = homogeneous; – = heterogeneous

Column-4: Crystal size of sintered WC-particles compared to grain size of WC-powders:
+ = large; – = small

two different lithium compounds namely LiOH and Li_3BO_3. While lithium borate dopant enhanced the stability of lithium to an extent that practically no Li-evaporation occurred, Li added as LiOH led to decrease in concentration of between 40 and 60% during 3 and 11 μm reduction conditions. Similar differences were found for

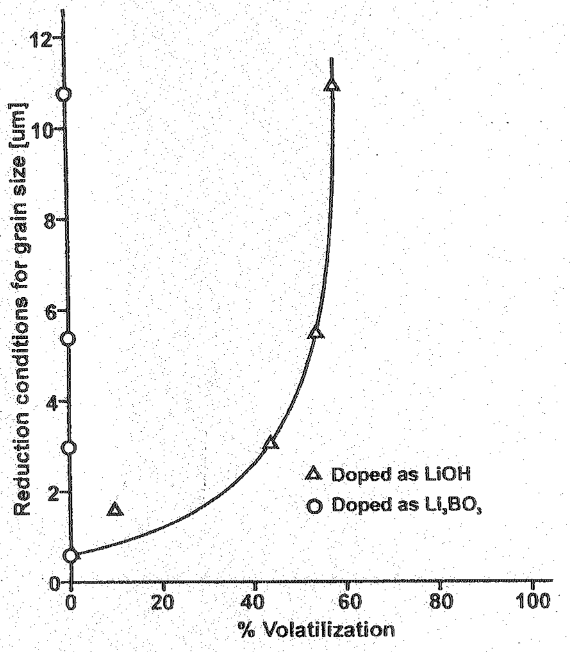

Fig. 1. Dependence of Li-evaporation rate on reducing conditions (starting concentration 100 ppm Na)

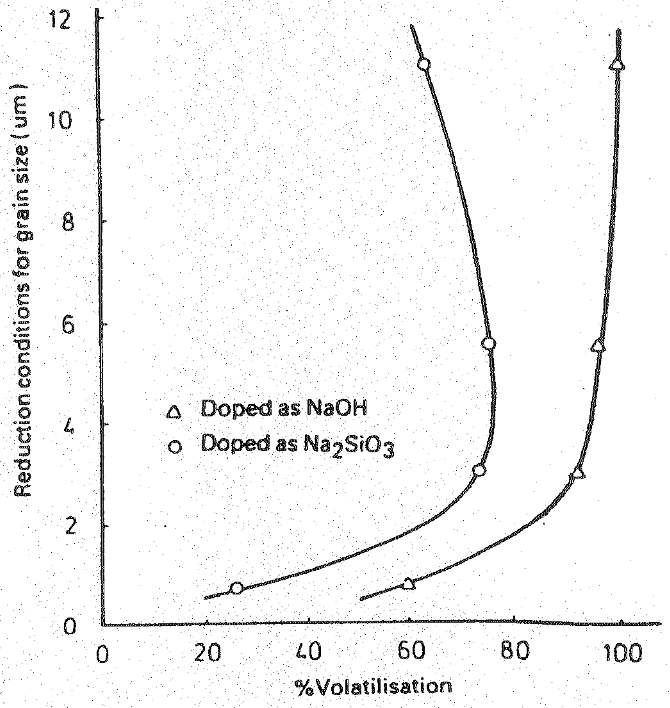

Fig. 2. (a) Dependence of Na-evaporation rate on reducing conditions (starting concentration 200 ppm Na)

sodium when doped as hydroxide or silicate respectively (Fig. 2) —sodium silicate being more stable than NaOH.

Increases of trace impurity, concentration during blue oxide reduction: Normally, an uptake of foreign elements should only be expected by diffusion of elements from the boat material into the tungsten powder. This reaction always takes place in certain time and temperature conditions and will not be dealt with here.

As shown above, sodium is rather volatile during reduction and sodium concentrations of some ppm are a usual contamination even for high purity tungsten oxide grades. During industrial tungsten reduction, excess hydrogen is applied and recirculated through different tubes of the furnace. For technical conditions leading to fine grain size tungsten powders of 0.5–1.5 μm, an increase in the sodium concentration was observed. The only possible explanation of this is that sodium is carried by the hydrogen stream from furnace chambers where finer W-powders at lower temperatures are produced. No explanation regarding the nature of the sodium compound being transported can be given at present.

Another contamination of fine tungsten powders was observed with carbon. Furthermore, seasonal dependence—in winter it was higher than in April or June was observed (Fig. 2b). The recirculated hydrogen passes a water seal supplied with river water. The carbon dioxide concentration in this water depends on the season due to the temperature-dependence of carbon dioxide solubility. Higher solubility of carbon dioxide in cold water during winter thus results in a higher concentration of carbon dioxide in hydrogen and causes an increase of carbon in fine tungsten powders.

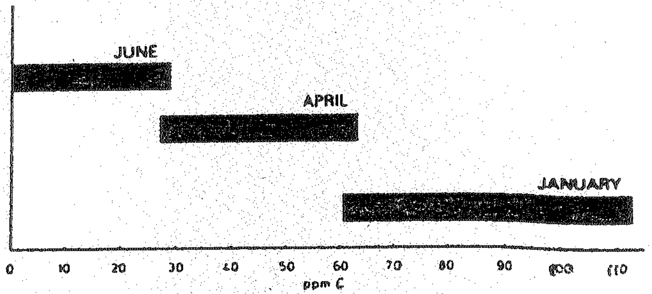

Fig. 2. (b) Seasonal dependence of the carbon content of 1 μm W-powder

Carbon diffusion rate: It is well known that even under constant carburizing conditions, differences in carbon diffusion velocity from one batch to the next sometimes occurred. In certain cases, an unusually high content of free carbon was found.

Our experiments revealed alkali metals to be responsible for a distinct retarding effect on carbon diffusion into the tungsten or tungsten carbide grains. This effect is concentration dependent. Other elements reacting with alkali metals like boron, silicon or phosphorus decrease this effect considerably, *e.g.*, 10 pm sodium in tungsten powder (200 ppm added to blue oxide as sodium hydroxide) gave a free carbon content of 0.13% whereas 64 ppm sodium in the presence of 100 ppm silicon (doped as sodium silicate) showed only 0.04% free carbon. 24 ppm lithium

(50 ppm doped as lithium hydroxide) showd 0.22% free carbon. Here also, as mentioned above, monoatomic carbide layers at the tungsten-gas-interface can be assumed to be responsible for this effect.

Influence of trace elements on tungsten carbide-grain growth during sintering of cemented carbide

Behaviour of fine tungsten carbide powders: Semi-quantitative results of metallographic examination of WC-grain growth during sintering of tungsten carbide 10% Co cemented carbide samples are shown in Columns 11 and 12 of Table-2. Doping elements can influence continuous and discontinuous grain growth of tungsten carbide crystals during liquid phase sintering. An effect of impurities on the tungsten carbide-grain growth during liquid phase sintering is much greater than the influence of the small variation in grain size and grain size distribution existing between different tungsten carbide powders: (1) A grain growth inhibiting influence could be observed with alkali metals, nickel, uranium and tin additions. (2) Fairly homogeneous structures were found when sodium hydroxide or sodium silicate dopings used. (3) Discontinuous or excessive local grain growth was originated by barium, aluminium, silicon, boron, phosphorus, zinc, copper and a combination of arsenic/antimony/bismuth.

It is interesting to note that alkali metals in concentrations of 10–50 ppm cause similar effects as those described earlier for carburization kinetics, as these elements also reduce the rate of tungsten carbide-grain growth during liquid phase sintering.

Discontinuous or excessive local grain growth always seems to be related to the presence of large polycrystalline tungsten carbide-agglomerates ranging between 10 and 80 μm. These particles, called pseudomorphous, originate from APT-crystals, or fragments thereof, which survive all the process steps from reduction to carburization (Figs. 3–6). They act, as known from large tungsten carbide-particle additions during sintering, as seed crystals (columns 13–16 in Table-2) which, due to Ostwald ripening, become growth centres for comparatively rapid tungsten carbide-grain growth.

Fig. 3. 5 μm tungsten powder, showing well developed low index cubic crystals (SEM x3000)

Fig. 4. Growth steps on tungsten crystal faces (SEM x6000)

Fig. 5. Al-doped 2.2 μm tungsten powder seen with SEM

In particular, powders containing phosphorus, boron, aluminium, silicon or arsenic/antimony/bismuth showed such excessive local grain growth. These tungsten carbide powder grades also showed extraordinarily high concentrations of the above mentioned coarse pseudomorphous particles (column 13 in Table-2). Some typical examples of micro-structures are given in Figs. 6–10.

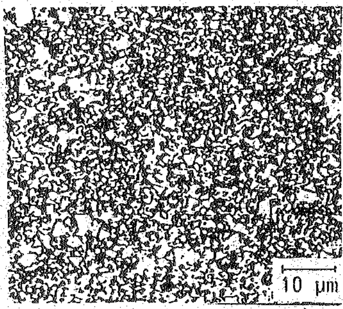

Fig. 6. Microstructure WC + 10% wt Co (without doping)

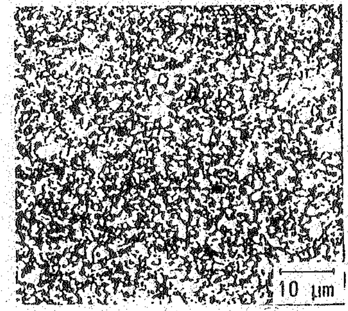

Fig.7. Microstructure WC + 10% wt Co: 200 ppm Na added to blue oxide, more uniform structure than undoped by grain growth inhibiting effect of Na

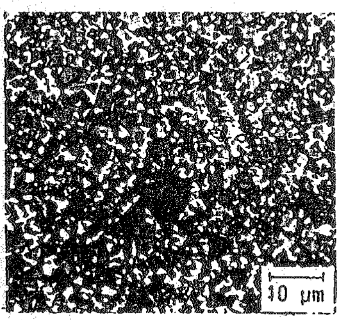

Fig. 8. Microstructure WC + 10% wt Co: sodium silicate doped, continuous grain growth caused by Si

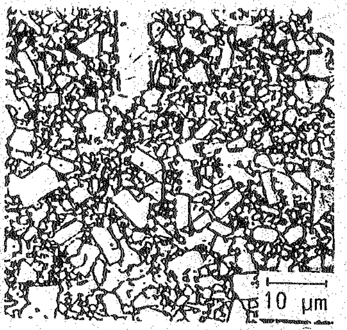

Fig. 9. Microstructure WC + 10% wt Co: Al-coped, discontinuous and continuous grain growth

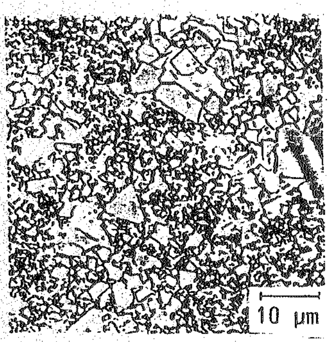

Fig. 10. Microstructure WC + 1% wt Co: *p*-doped, discontinuous grain growth

This leads furthermore to the conclusion that certain dopants cannot be distributed homogeneously when mixed with blue oxide. They are possibly enriched in some distinct particles and thus cause the stability of the pseudomorphous particles. So far we do not have any other explanation. Direct experimental proof of such local increases in doping element concentrations by micro-probe techniques cannot be made due to the relatively low sensitivity of X-ray detection devices in a heavy element matrix like tungsten.

Behaviour of coarse tungsten carbide powders and influence of impurities: Although all the tungsten powders were prepared under the same reduction conditions which normally lead without dopants to a 5.5 μm tungsten powder. Table-3 shows that all the alkali metal doped samples, due to the grain growth enhancing effect of these metals during reduction, resulted in much coarser tungsten carbide grades of about 15–15 μm. All the other powders were around 5.5 μm as expected.

Tungsten powders doped with boron, aluminium (Fig. 11) or uranium showed much smaller tungsten carbide crystal sizes after carburization than undoped tungsten powder of the same size (Fig. 12). On the contrary, the elements magnesium, zinc, phosphorus (Fig. 13) and tin enhanced the single crystalline tungsten carbide grain size in cemented carbides.

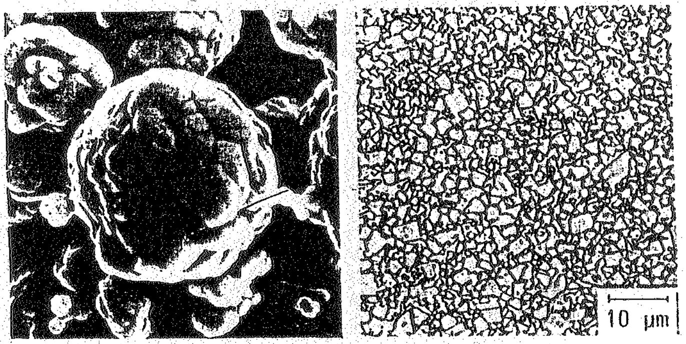

Fig. 11. SEM micrograph of Al-doped coarse tungsten carbide and corresponding tungsten carbide + 10% wt Co microstructure

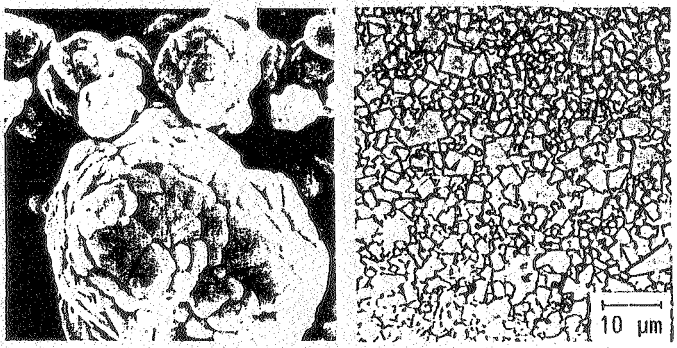

Fig. 12. SEM micrograph of undoped coarse tungsten carbide and corresponding tungsten carbide + 10% wt Co microstructure

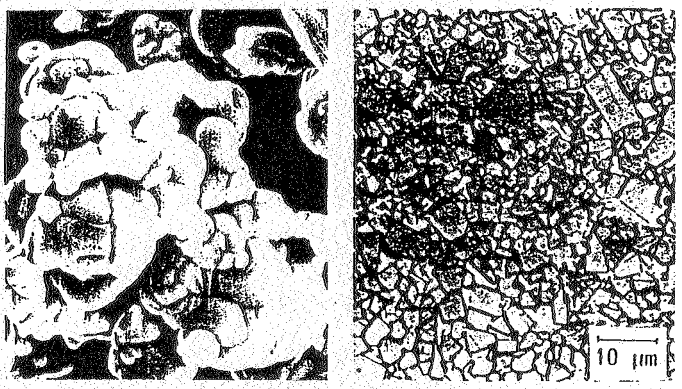

Fig. 13. SEM micrograph of *p*-doped coarse tungsten carbide and corresponding tungsten carbide + 10% wt Co microstructure

Comparing columns 11 and 14 in Table-3, a relationship can be seen between the size of single crystalline domains of tungsten carbide particles and the tungsten carbide grain size in the sintered structure.

(a) The smaller the single crystalline domains in the tungsten carbide powders, the less tungsten carbide grain growth observed during liquid phase sintering.
(b) Tungsten carbide powder having single crystalline domains which were different in size resulted in a more non-uniform grain size distribution after sintering.

The following example shows that all this is really a consequence of the minute amount of dopants added to the blue oxide. Figs. 14 and 15 show tungsten carbide powders doped with 200 and 50 ppm lithium respectively and the corresponding structure of tungsten carbide-10% Co samples after sintering. In the tungsten carbide powder stage the respective lithium concentrations were still measurable and distinguishable by analytical methods (154 and 24 ppm). After carburization, however, the lithium concentration was below the analytical determination limit of 10 ppm in both cases.

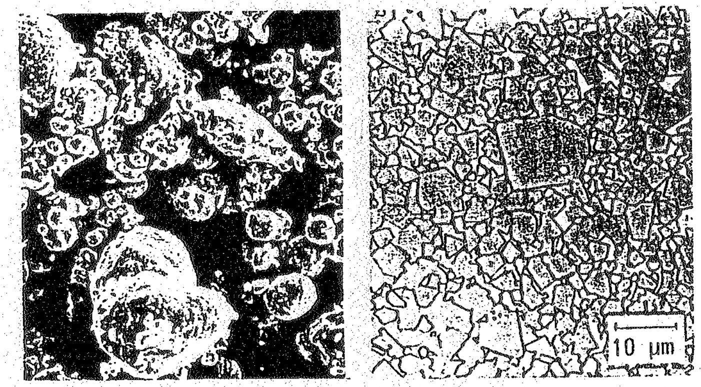

Fig. 14. SEM micrograph of 200 ppm Li-doped coarse tungsten carbide and corresponding tungsten carbide + 10% wt Co microstructure

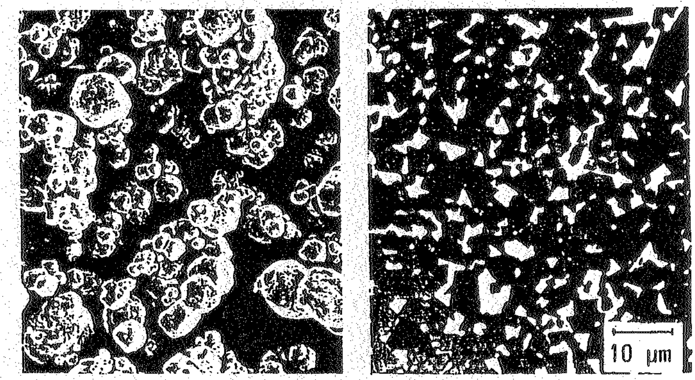

Fig. 15. SEM micrograph of 50 ppm Li-doped tungsten carbide and corresponding tungsten carbide + 10% wt Co microstructure

It is clear from the different single crystalline sizes in the tungsten carbide powder stage and the differences in the micro structure of tungsten carbide/Co after sintering, that there must be a difference in the lithium concentration between the two samples and, consequently, lithium concentrations as low as less than 10 ppm still have an effect on the tungsten carbide-grain growth during liquid phase sintering. A possible explanation for the effectiveness of such small amounts would be that mono-atomic layers exist at the interphase tungsten carbide/liquid cobalt which block there the transfer mechanism of tungsten and carbon atoms.

Effects of trace elements on some technological properties of tungsten and tungsten carbide powders

Tungsten powder: Due to the influence of traces of foreign elements on reduction kinetics, the characteristics of the resulting tungsten powders are also changed. These changes in powder properties will cause variations in compacting and sintering behaviour due to the changes in technological properties such as green density and green strength of compacts and shrinkage during sintering. These properties are of great and direct importance for solid state and liquid phase sintering as applied in the production of ductile tungsten or heavy metal materials[7].

Although tungsten powder is only an intermediate in cemented carbide production, tungsten powder properties nevertheless partly influence the quality of the corresponding tungsten carbide powder, thus influencing the sintering behaviour and the properties of cemented carbides, too.

Agglomeration and strength of agglomerates (Column 14 in Table-2, Column 15 in Table-3): The degree of agglomeration is defined as difference between the average grain size as supplied and the average grain size after deagglomeration expressed in per cent of the as supplied value. Fig. 16 shows the usual dependence of this difference on the grain size as supplied. It is between 7 and 10%. Foreign elements, doped into blue oxide or already present therein, can influence the degree of agglomeration remarkably.

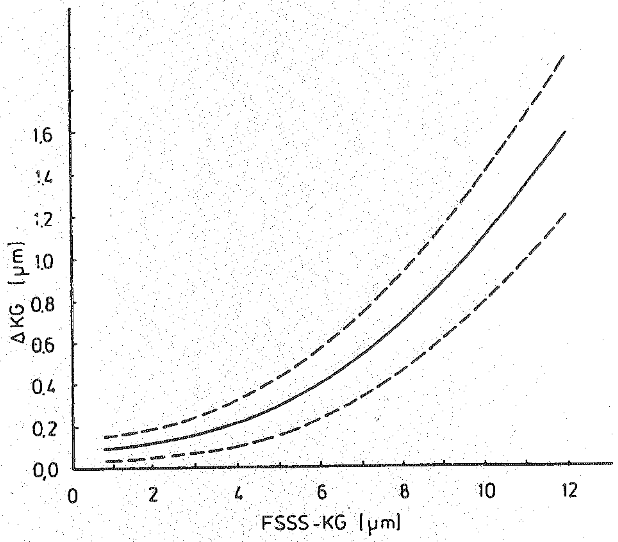

Fig. 16. Dependence of agglomeration on as-supplied grain size

Typical elements which increase the degree of agglomeration and originate connections of high strength between tungten crystallites, are the alkali metals. It is known from literature[2, 3] that during reduction of alkali tungstates, tungsten bronzes, having a reduced oxygen content, are formed as intermediates. Their melting points lie in the range of the reduction temperatures.

Tungsten-particles were first soldered together by these molten bronzes formed at their surface. During the later stages of tungsten reduction, these bronzes are decomposed and completely reduced by hydrogen to metallic tungsten and connections of high strengths are thus formed and remain. They cannot be destroyed by usual blending operations. The high coherence is probably due to formation of neck-like tungsten connections between tungsten crystallites as shown in Figs. 17 and 18. As seen from these figures, it proves the above assumption that molten areas on surfaces exist, because typical shrinkage cracks developed.

Fig. 17. Tungsten-powder reduced from 200 ppm Na-doped blue oxide seen with SEM

Fig. 18. Tungsten-powder reduced from 200 ppm Li-doped blue oxide seen with SEM

An example of a typical element decreasing the degree of agglomeration is aluminium. This can already be observed on sub-micron tungsten powders by comparison of undoped and aluminium-doped samples (Figs. 19 and 20). For larger grain size tungsten powders, this effect is even more pronounced (Figs. 6 and 7), where existing connections between tungsten grains are loose. As known from the literature[11, 12], aluminium hinders the formation of tungsten bronzes. Therefore, high strength connections between tungsten particles as described above do not develop, even in the presence of small amounts of alkaline metals.

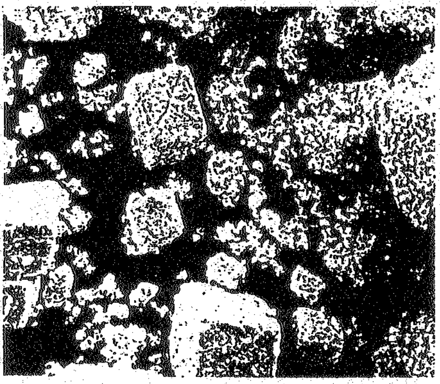

Fig. 19. Submicron tungsten powder of high purity (0.55 μm) seen with SEM

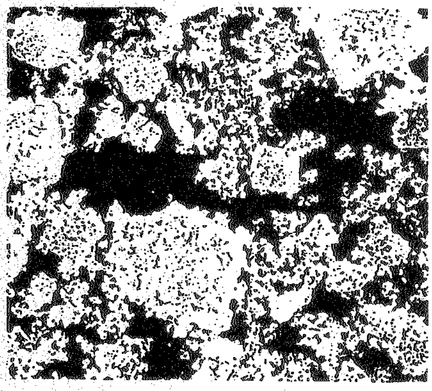

Fig. 20. Al-doped submicron tungsten powder seen with SEM (0.5 μm)

Scott density: Tungsten powders always show a certain degree of agglomeration due to the CVT-reaction responsible for grain growth. As with all other metal powders, there exists a linear relationship between grain size and Scott density for tungsten too. Any unusual degree of agglomeration influences this relationship. According to the foregoing discussions, alkali metal-doped samples should result in a tungsten powder having lower Scott density whereas aluminium-doped powders should show higher Scott density than normal tungsten powder. Column 16 in Tables 2 and 3 proves this statement.

Grain size distribution: In principle, the blue oxide powder layer height in the reduction boat is closely linked to the tungsten grain size as well as for the grain size distribution. As discussed in the earlier section dealing with the behaviour of various impurities during reduction of tungsten blue oxide, water vapour concentration within the powder layer regulates the grain growth. This concentration is always lower at the surface of the powder layer due to the hydrogen gas stream passing over the boat. The water vapour concentration increases steadily from the surface to the bottom where it is at its maximum. The residence time of the water will also be longer at the bottom than at the surface. The water vapour concentration gradient in combination with the prolonged reaction time will correspondingly provoke a certain spread in the tungsten powder grain size (column 18 in Tables 2 and 3). This means in practice that the higher the powder layer, the broader the grain size distribution.

Thus, foreign elements may only influence grain size distribution on elements enhancing grain growth. In the presence of such substances the powder layer height has to be reduced—in comparison with undoped oxide—in order to obtain the desired grain size under otherwise equal reaction conditions. This opens up a possibility of producing tungsten powder having closer grain size distributions at comparable average grain size.

Tungsten carbide powders; The properties of tungsten carbide powders depend to a large extent on the properties of their corresponding tungsten powders and, of course, on the carburization conditions.

Agglomeration: Theoretically, agglomeration of tungsten carbide particles is originated by strong connections which already exist between tungsten particles and which can survive carburization.

At surfaces (high temperature carburized tungsten having large single crystalline domains) a more homogeneous coarse cemented carbide structure results. The higher the amount of surfaces originally covered with impurities and the amount of grain boundary fracture surfaces (high amount of impurities causing small single crystalline domains) is, the more heterogeneous the sintered cemented carbide structure will be.

It is clear that not only the microstructure is influenced by such impurities, it can be reasonably expected that the fine grain boundary strength of sintered samples will be influenced by impurities present at the interface. Again, further experiments are needed to confirm this opinion.

REFERENCES

1. H. Schulze-Schreiber, *Int. Powder Metall. (Florence)* (1992).
2. G. Jangg, 10th Plansee Seminar (1991).
3. J. Neugenbauer, *Planseeber. Pulvermet.*, **23**, 77 (1985).
4. S. Yamazaki, *Planseeber. Pulvermet.*, **22** (1984).
5. T. Ekstrom and R.J.D. Tiliey, *Chemica Scripta*, **16**, 1–23 (1990).
6. H. Mayer, 10th Plansee Seminar (1991).
7. E. Lassner, 10th Plansee Seminar (1991).
8. M. Schreiner, 10th Plansee Seminar (1991).
9. T. Schmitt, M. Schreiner, Blux (to be published).
10. E. Alizadeh, Thesis, Tuwien (1983).
11. E. Lardner, *Powder Metallurgy*, **13**, 394 (1990).
12. Gemelins Handbuch der Anorg. Chemie Wofram No. 54 (1993).

(*Received*: 30 December 2004; *Accepted*: 9 May 2006) AJC-4902